Adiabatic stabilization of excitons in intense terahertz laser

Ren-Bao Liu and Bang-Fen Zhu
Center for Advanced Study, Tsinghua University, Beijing 100 084, People's Republic of China

High-precise calculation of near-infrared absorption and transient spectra in bulk semiconductors irradiated by an intense terahertz (THz) laser shows that, the ionization rate of the ground-state exciton, probed through the dynamic Fano resonance, may decrease with the increase of the THz laser intensity. This counterintuitive effect indicates the excitons are stabilized against the field-ionization. The much lower Rydberg energy and "atomic unit" of laser intensity for excitons, and the possibility of creating excitons from the "vacuum state" allow observing the excitonic stabilization in experiments, in contrast to the case of atomic stabilization.

PACS numbers: 71.35.Cc, 78.20.Jq, 32.80.Fb, 42.50.Md

arXiv:cond-mat/0109038v1 4 Sep 2001

In accordance to Einstein's theory of the photoelectric effect, an electron can be stripped from its atom by light beams with sufficiently high frequency. As the intensity of a light beam is increased, the stripping probability of the electron increases owing to the increasing number of photon impacts. Surprisingly, since the late 1980's, theoretical investigations and numerical simulations [1–6] have predicted that when the electric field, associated with a laser of sufficiently high intensity and frequency, approaches or exceeds the electrostatic field between the electron and the ion in an atom, the wave function of the irradiated atom may be distorted adiabatically into a distribution with two well separated peaks. The peak spacing increases with increasing the field intensity, thus the atomic electron spends more time far away from the nucleus, and the ionization rate slows down dramatically till almost totally suppressed. In other words, the adiabatic stabilization of the atom occurs.

The observation of this atomic stabilization effect is, however, extremely difficult. Firstly, for the atomic ground state, the high-frequency and high-intensity condition requires an extreme ultraviolet laser with intensity larger than an atomic unit ($\sim 3.51\times10^{16}$ W/cm^2), which seems not available in the near future. Secondly, and more vitally, sufficiently slow turn-on is demanded for the laser pulse to adiabatically drive the atomic ground state into a stable dressed state; during the rise time of the super-intense laser pulse, however, substantial ionization has already been inevitable [7], which prevents the effect from observation. Some researchers even argued that it was impossible to observe such an adiabatic stabilization of atoms [8,9]. In fact, except for a few disputable indications for the stabilization of high Rydberg states [10], so far there is no unambiguous experimental evidence for the atomic stabilization.

It is compelling to settle the debate whether this effect exists or not. Apart from the pure curiosity in basic research, the atomic stabilization is also of importance in potential application, such as the high harmonic generation [11] and quantum computation [12], as it can quench the undesired ionization and dephasing caused by the intense laser that is used to drive electrons or to manipulate a qubit in an atom.

In this Letter, we report on the adiabatic stabilization of hydrogen-atom-like excitons in semiconductors. The excitonic stabilization (XS), in contrast to its atomic counterpart, is definitely an observable effect, owing to the basic characteristic of excitons that they are created from "vacuum" of carriers by the interband optical excitation. In our study, the dressed exciton states are prepared by weak near-infrared (NIR) laser pulses in semiconductors in the presence of a quasi-continuous terahertz (THz) field, as in most recent experiments on the dynamical Franz-Keldysh effect [13–15]. The ionization rate or lifetime of the dressed excitons can be directly extracted by monitoring either the linewidth of absorption peaks or the decay time of transient signals. Thus the "turn-on" problem is safely circumvented as long as the pulsed interband excitation and the following dephasing process of excitons are well covered by the flattop region of the THz laser pulse.

Moreover, the present laboratory gear is already ready for observing the XS effect. Due to the small effective mass μ and large dielectric constant ε, an exciton has much smaller binding energy E_B than the hydrogen atom does, and the "excitonic unit" for laser intensity ($\propto \mu^4/\varepsilon^{5.5}$) in a typical semiconductor like GaAs is about 10 orders of magnitude smaller than the atomic unit. So, the "high-intensity and high-frequency" requirement for the XS can readily be fulfilled by the free-electron lasers operating with MW/cm^2 power and THz frequency [16].

Our investigation is based on the high-precise calculation of interband optical spectra, which includes properly the Coulomb interaction, the nonperturbative ac-field, and the contribution of continuum states. To avoid unnecessary complexity, the excitonic state is treated within the simple effective-mass approximation. Then the motion equation for the relative motion of an electron-hole

pair is

$$i\hbar\partial_t\psi(\mathbf{r},t) = (\hat{H} - i\gamma_2)\psi(\mathbf{r},t) + \chi(t)e^{-i\Omega_0 t}\delta(\mathbf{r}), \quad (1)$$

$$\hat{H} \equiv E_g - \frac{\hbar^2}{2\mu}\nabla_{\mathbf{r}}^2 - \frac{e^2}{4\pi\varepsilon r} + eFz\cos(\omega t), \quad (2)$$

where E_g is the band gap, F is the field strength of the THz laser associated with frequency ω and linearly polarized in the $\mathbf{z}$ direction, $\chi(t)$ denotes the NIR pulse excitation centered at Ω_0, and γ_2 is an interband dephasing-rate due to phonon scattering. The THz laser is assumed in a continuous wave (cw) form, because its microsecond duration [16] is much longer than the picosecond interband excitation and dephasing process. This model system is mathematically equivalent to a hydrogen atom in an intense laser except that the electron-hole pair is generated by the NIR laser.

Without the Coulomb coupling, the eigensolution of the time-dependent Hamiltonian (Eq. (2)) is the Volkov state [17], which, as the basis set, reads

$$|\mathbf{k}, m\rangle = e^{im\omega t - ia_F k_z\cos(\omega t) + i\frac{U_p}{2\hbar\omega}\sin(2\omega t)}|\tilde{\mathbf{k}}\rangle,$$

where m and $\mathbf{k}$, associated with quasienergy $\varepsilon_{\mathbf{k}m} = \frac{\hbar^2k^2}{2\mu} + U_p + m\hbar\omega$, denote the sideband index and the wavevector, respectively. Here $U_p \equiv \frac{e^2F^2}{4\mu\omega^2}$ is the effective ponderomotive potential, $a_F \equiv \frac{eF}{\mu\omega^2}$ is the classical excursion amplitude of an electron in the ac-electric field, and $|\tilde{\mathbf{k}}\rangle$ is the Bloch-state with accelerating quasimomentum $\mathbf{k} - \frac{eF}{\hbar\omega}\hat{\mathbf{z}}\sin(\omega t)$. With the excitonic Rydberg unit adopted, the matrix elements of the Coulomb potential read

$$V_{\mathbf{k}+\mathbf{q}m+n,\mathbf{k}m} = -\pi^{-2}q^{-2}i^n J_n(a_F q_z),$$

where $J_n(x)$ denotes the nth-order Bessel function of the first kind. The intra-sideband ($n = 0$) interaction is directly related to the Kramers-Hennerberg (KH) potential, the time-average of the Coulomb potential in the coordinate frame rested on the quivering electron [18]. The KH potential has logarithmic singularity in the segment between the turning points $\pm\hat{\mathbf{z}}a_F$ and $r^{-1/2}$ singularity at the ends. Consequently, the ground state $|\Phi\rangle$ is stretched along the segment of singularity and becomes dichotomous for super-intense field ($a_F \gg a_B$, the exciton Bohr radius) [1].

The spectrum of the system exhibits the sideband structure. As illustrated in the lower inset in Fig. 1, each sideband consists of several discrete states and a continuum, and the discrete states are embedded in the ionization continua of lower sidebands. As predicted very recently in an ac-driven biased semiconductor superlattice [19], the quantum interference between a discrete state of quasienergy excitons and the degenerate continuum of a sideband can lead to the dynamic Fano resonance (DFR), which manifests itself as broadened asymmetric lineshape in absorption spectra and as intrinsic decay in transient four-wave mixing signals. Thus, the ionization rate of the quasi-bound Floquet-state excitons and the XS effect can be studied via the DFR induced by the inter-sideband coupling ($n \neq 0$) in the present system.

To calculate the time-dependent wavefunction, we numerically integrate Eq. (1) in the cylindrical polar coordinates by extending the space-time difference method [20] to a time-periodic system, with the initial condition as $\psi(\mathbf{r}, -\infty) = 0$. The out-going waves are absorbed at the boundary with the mask technique [4]. The NIR absorption spectrum $\alpha(\Omega) \propto \Im\big[P(\Omega)/\chi(\Omega)\big]$, in which $P(t) \equiv \psi(\mathbf{0}, t)$ gives directly the transient interband polarization (i.e. coherence). In the calculation, $\hbar\omega = 10$ meV (~ 2.4 THz), $\gamma_2 = 1$ meV, and the NIR pulse is assumed to be of a Gaussian shape, i.e. $\chi(t) = \chi_0 \exp\left(-t^2/2\tau^2\right)$. For cw absorption, τ is taken as $8/\omega$, which is large enough to eliminate the sideband overlap. The material parameters take bulk GaAs as an example ($E_B = 4$ meV and $a_B = 10$ nm).

Figure 1 plots the NIR cw-absorption spectra of the bulk GaAs driven by the THz-field with various strength. The blue-shift of the peak associated with the $1s$ exciton state results mainly from the effective ponderomotive energy U_p and additionally from the decrease of the binding energy $\mathcal{E}_B$. The sideband structure of the Floquet-state exciton is visible in the spectra, and particularly, for $F > 24$ kV/cm, or the intensity $I > 2.3$ MW/cm^2 [21], the -1ω sideband can be stronger than the 0ω one that evolves from the original $1s$ state. There is also significant absorption in the band gap. Indeed, the dynamical Franz-Keldysh effect [15] is properly reproduced in this high-precise calculation, and the result can be well understood in the Floquet-state picture.

The exciton ionization rate is probed through the broadening and distortion of absorption peaks in the NIR-spectra. As displayed in the inset, the asymmetric resonance peak is well fitted with the Fano lineshape [22] characterized by the shape parameter q and broadening constant γ

$$\alpha(\Omega) = \alpha_0 + \alpha_1\frac{(q\gamma + \Omega - E_g + \mathcal{E}_B)^2}{\gamma^2 + (\Omega - E_g + \mathcal{E}_B)^2},$$

indicating the occurrence of the DFR. By fitting the 0ω peak, the ionization rate Γ can be extracted via $\gamma \approx \gamma_2 + \Gamma/2$. As shown in Fig. 2, γ (hence the ionization rate) increases with the laser intensity until $F \approx 16$ kV/cm (correspondingly, $I \approx 1.0$ MW/cm^2 [21] and $a_F \approx 1.28a_B$). Beyond that critical field strength, the ionization rate commences to decrease, and approaches zero at $F \approx 28$ kV/cm, clearly demonstrating the XS effect.

Γ can also be obtained analytically in the high-frequency approximation [23]. When the wavefunction dichotomy is negligible for medium a_F (say $a_F < 3a_B$),

a compact result for Γ of the ground state [23] can be derived as

$$\Gamma \approx \sum_{n\omega>\mathcal{E}_B} \frac{32\pi}{k_n^3} \left| \int_{-a_F}^{+a_F} \frac{\Phi(\mathbf{z})dz}{2a_F} \right|^2 \int_0^1 J_n^2(a_F k_n x)dx,$$

where $k_n^2 = n\omega - \mathcal{E}_B$. When field is enhanced so that $a_F k_n$ approaches or exceeds 1, due to rapid oscillation of the Bessel function, the integration over x diminishes. Physically, this originates from the destructive interference of the out-going waves scattered from different part of the initial state. On the other hand, the stretching of the state along the field will reduce the wavefunction peak, contributing additionally to the XS.

Fano interference is one of fundamental channels for irreversible decay [24,25], so the XS can also be directly observed in the time domain by monitoring the transient optical signal after a pulsed excitation. The time-resolved interband polarization is calculated for several THz-field strengths and plotted in Fig. 3. The duration of the NIR pulse τ is then set to be $2/\omega$, and the central frequency is chosen for each field strength to be resonant with the brightest transition, namely $\Omega_0 - E_g = -4$, -2, 2, 5, and 6 meV for $F = 0$, 8, 16, 20, and 30 kV/cm, respectively. To single out the dephasing induced by the DFR only, the reformulated signal $\mathcal{P}(t) \equiv P(t)\exp(\gamma_2 t)$ is plotted. At finite field, the optical signal roughly oscillates with the period of $T \equiv 2\pi/\omega$, because the states in the KH potential oscillate periodically in the laboratory frame. The modulation beat superimposed on the fast oscillation results from the quantum interference between the Floquet states with different quasienergy. The dynamic Fano interference between the discrete state and the continuum opens a new channel for interband dephasing, leading to the decay of the transient signal. The XS effect is verified by the fact that the dephasing rate calculated for $F > 16$ kV/cm begins to decrease, consistent with the variation trend of the ionization rate as shown in Fig. 2. For $F = 30$ kV/cm ($I \approx 3.6$ MW/cm^2 [21]), the decay of the signal almost disappear. To measure the transient signals, nonlinear optical experiments like four-wave mixing are usually adopted, in which many-body correlation is important sometimes [26] and may induce new interesting effects on XS, which, however, is out of the scope of our present study.

Fig. 4 displays snapshots of the probability distribution of the exciton wavepacket resonantly excited by a pulse ($\Omega_0 - E_g = 8.88$ meV) with $\tau = 20/\omega$, corresponding to the spectral width 0.5 meV. When the NIR-excitation pulse is over, the wavepacket performs almost perfect periodic swinging along the $z-$axis with the turning points located at about $\pm\hat{\mathbf{z}}a_F$, except for an overall exponential decay due to the ionization. This periodic behavior is verified by the time-dependence of the optical signal (see the inset). Because of the inter-sideband mixing, the wavepacket shape varies drastically within a period, in contrast to the unchanged shape of the periodically oscillating wavepacket in the KH potential without inter-sideband coupling [1]. All these demonstrate that a quasi-bound Floquet state is formed in the strong THz-field, and justify our ascribing the suppression of the Fano broadening and dephasing rate to the adiabatic XS.

In summary, the novel excitonic stabilization effect, a counterpart of the atomic stabilization effect, has been predicted and explored nonperturbatively in a coupled system of semiconductors and intense THz-fields by high-precise calculation.

This work was supported by the National Science Foundation of China, and R.B.L was also supported by China Postdoctoral Science Foundation.

[1] M. Pont, N. R. Walet, M. Gavrila, and C. W. McCurdy, Phys. Rev. Lett. **61**, 939 (1988); M. Pont, N. R. Walet, and M. Gavrila, Phys. Rev. A **41**, 477 (1990).
[2] M. Pont and M. Gavrila, Phys. Rev. Lett. **65**, 2362 (1990).
[3] Q. Su, J. H. Eberly, and J. Javanainen, Phys. Rev. Lett. **64**, 862 (1990).
[4] K. C. Kulander, K. J. Schafer, and J. L. Krause, Phys. Rev. Lett. **66**, 2601 (1991).
[5] M. Dörr, R. M. Potvliege, D. Proulx, and R. Shakeschaft, Phys. Rev. A **43**, 3729 (1991).
[6] J. H. Eberly and K. C. Kulander, Science **262**, 1229 (1993).
[7] P. Lambropoulos, Phys. Rev. Lett. **55**, 2141 (1985).
[8] S. Geltman, Chem. Phys. Lett. **237**, 286 (1995).
[9] C. Figueira de Morisson Faria, A. Fring, and R. Schrader, J. Phys. B **31**, 449 (1998).
[10] M. P. de Boer, J. H. Hoogenraad, R. B. Vrijen, L. D. Noordam, and H. G. Muller, Phys. Rev. Lett. **71**, 3263 (1993); N. J. van Druten, R. C. Constantinescu, J. M. Schins, H. Nieuwenhuize, and H. G. Muller, Phys. Rev. A **55**, 622 (1997).
[11] P. Salières, A. L'Huillier, P. Antoine, M. Lewenstein, in *Advances in Atomic, Molecular, and Optical Physics*, edited by B. Bederson and H. Walther (Academic Press, New York, 1999), Vol. **41**, p.83.
[12] B. E. Cole, J. B. Williams, B. T. King, M. S. Sherwin, and C. R. Stanley, Nature **410**, 60 (2001).
[13] J. Cêrne, J. Kono, M. S. Sherwin, M. Sundaram, A. C. Gossard, and G. E. Bauer, Phys. Rev. Lett. **77**, 1131 (1996).
[14] J. Kono, M. Y. Su, T. Inoshita, T. Noda, M. S. Sherwin, S. J. Allen, Jr., and H. Sakaki, Phys. Rev. Lett. **79**, 1758 (1997).
[15] K. B. Nordstrom, K. Johnsen, S. J. Allen, A.-P. Jauho, B. Birnir, J. Kono, T. Noda, H. Akiyama, and H. Sakaki, Phys. Rev. Lett. **81**, 457 (1998).
[16] G. Ramian, Nucl. Instrum. Methods Phys. Res. A **318**, 225 (1992).

[17] D. M. Volkov, Z. Phys. **94**, 250 (1935).
[18] H. A. Kramers, *Collected Scientific Papers* (North-Holland, Amsterdam, 1956), p.866; W. C. Henneberger, Phys. Rev. Lett. **21**, 838 (1968).
[19] R. B. Liu and B. F. Zhu, J. Phys.: Condens. Matter **12**, L741 (2000).
[20] S. Glutsch, D. S. Chemla, and F. Bechstedt, Phys. Rev. B **54**, 11592 (1996).
[21] Here we use the intensity inside the material with relative dielectric constant $\varepsilon/\varepsilon_0 = 9.0$. The vacuum value is larger by about 1.3.
[22] U.Fano, Phys. Rev. **124**, 1866 (1961).
[23] M. Pont, Phys. Rev. A **44**, 2141 (1991); **44**, 2152 (1991).
[24] U. Siegner, M.-A. Mycek, S. Glutsch, and D. S. Chemla, Phys. Rev. Lett. **74**, 470 (1995).
[25] C. P. Holfeld, F. Löser, M. Sudzius, K. Leo, D. M. Whittaker, and K. Köhler, Phys. Rev. Lett. **81**, 874 (1998).
[26] D. S. Chemla and J. Shah, Nature **411**, 549 (2001).

FIG. 1. Linear absorption spectrum for several THz-field strengths indicated by F. The upper-right inset shows, as an example, the Fano resonance fitting process for $F = 24$ kV/cm, where the squares are the fitted data. The lower-right inset shows schematically the sideband structure of the Floquet-state excitonic spectrum.

FIG. 2. Fano broadening constant versus the THz-field strength.

FIG. 3. Real-time dependence of the interband polarization for various THz-field strength indicated by F, in which the curves are offset for clarity. The intensity profile of the NIR pulse (the dotted curve) is also shown for comparison.

FIG. 4. Probability distribution of the NIR-pulse-excited wavepacket at several time instant within a period T for the THz-field of $F = 24$ kV/cm. The inset shows the semi-logarithmic plots of the intensity of the NIR pulse (dotted line) and transient interband optical signal ($|\mathcal{P}(t)|^2$, solid line) as functions of time, and the time snatch (marked by the bar) where the snapshots are made.

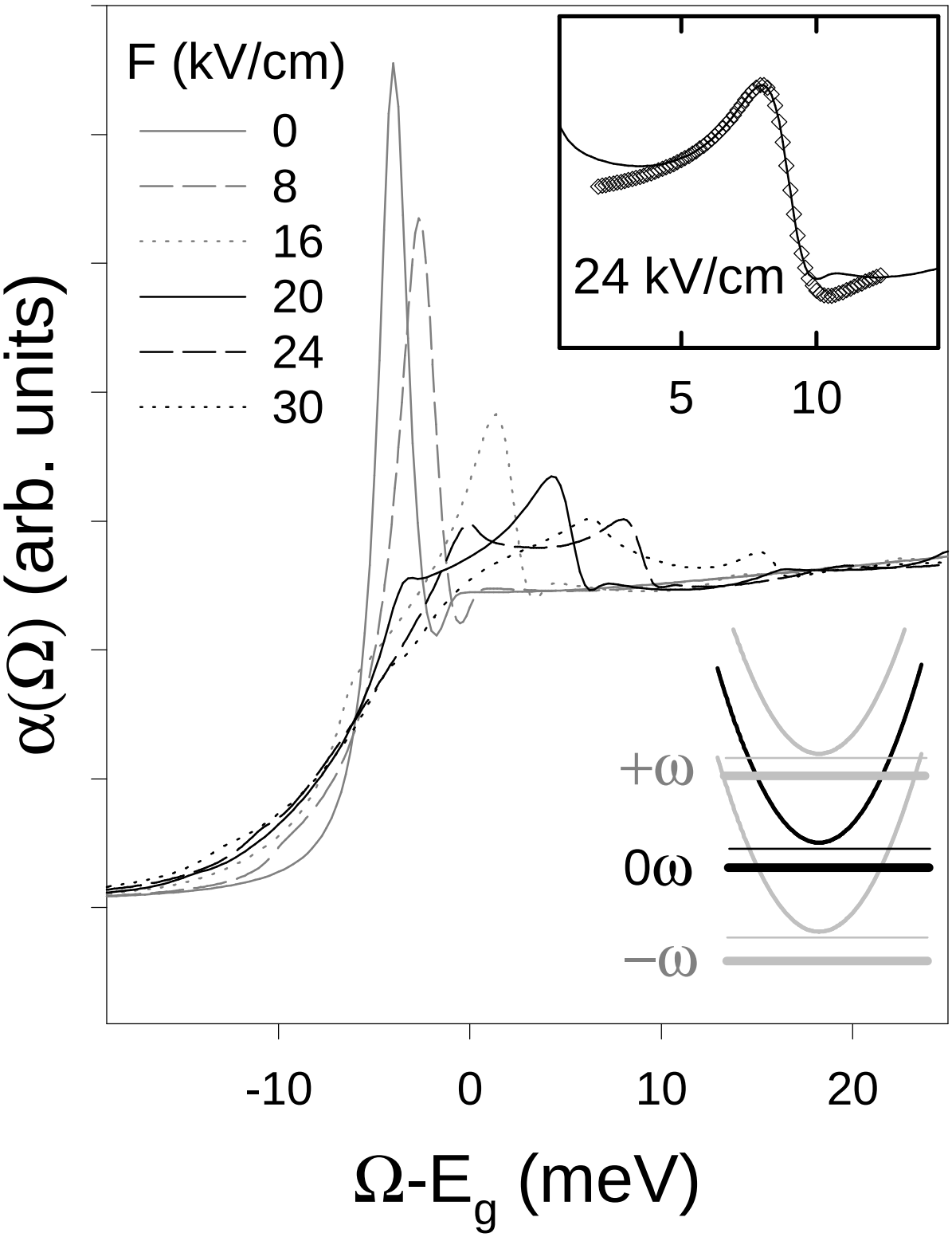
F (kV/cm)
0
8
16
20
24
30
24 kV/cm
5
10
+ω
0ω
−ω
α(Ω) (arb. units)
-10
0
10
20
Ω-E_g (meV)

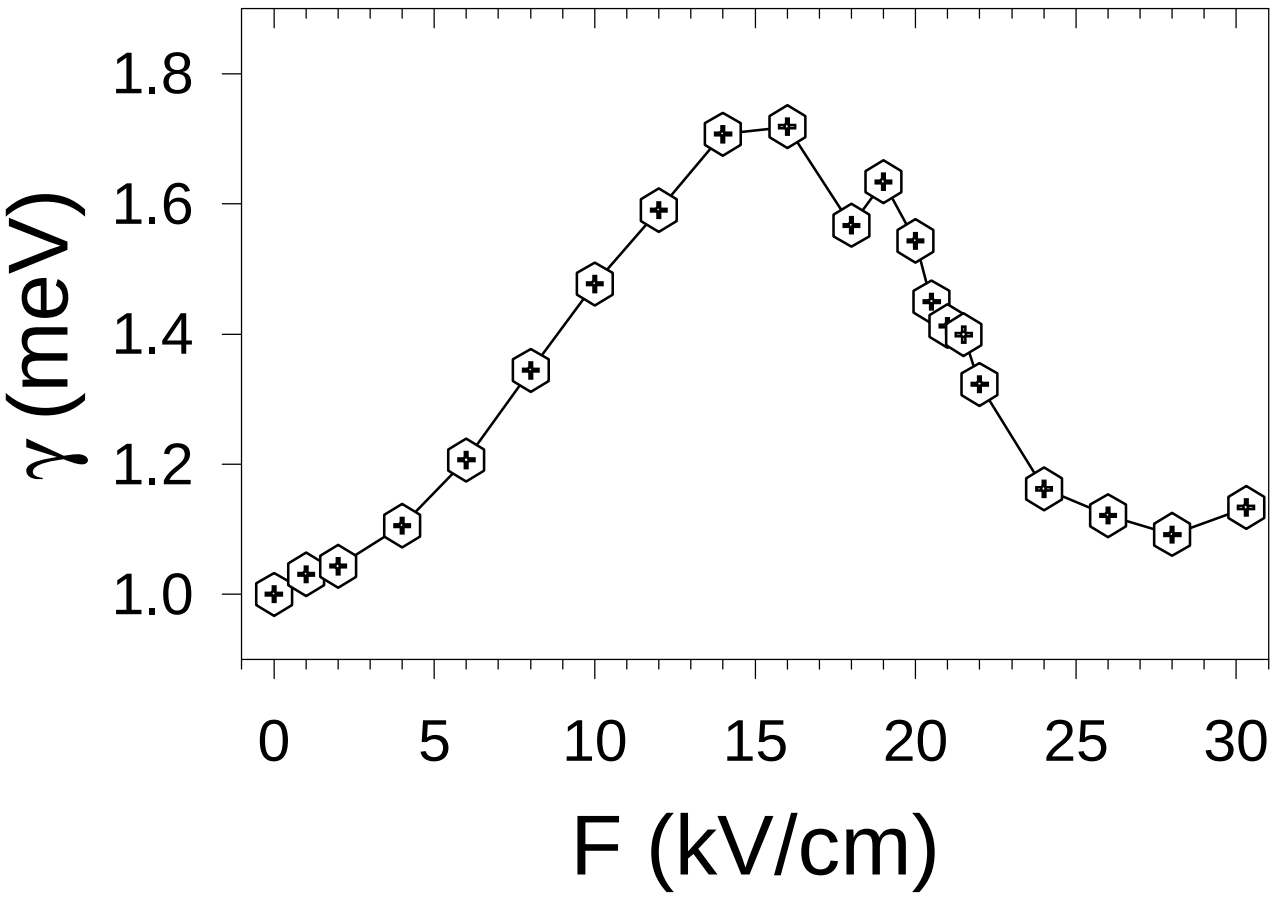
1.8
1.6
1.4
1.2
1.0
γ (meV)
0
5
10
15
20
25
30
F (kV/cm)

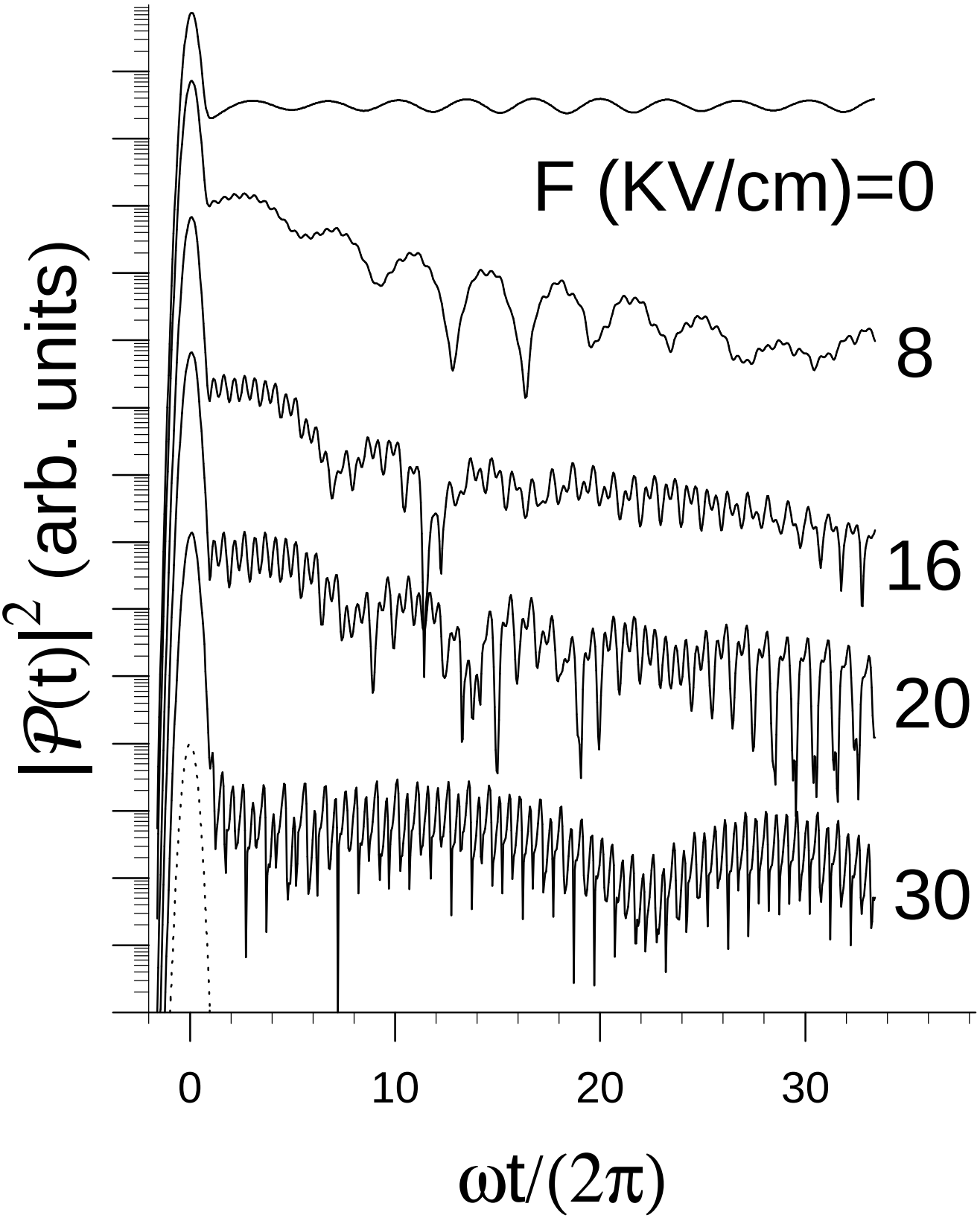
F (KV/cm)=0
8
16
20
30
$|\mathcal{P}(t)|^2$ (arb. units)
0
10
20
30
$\omega t/(2\pi)$

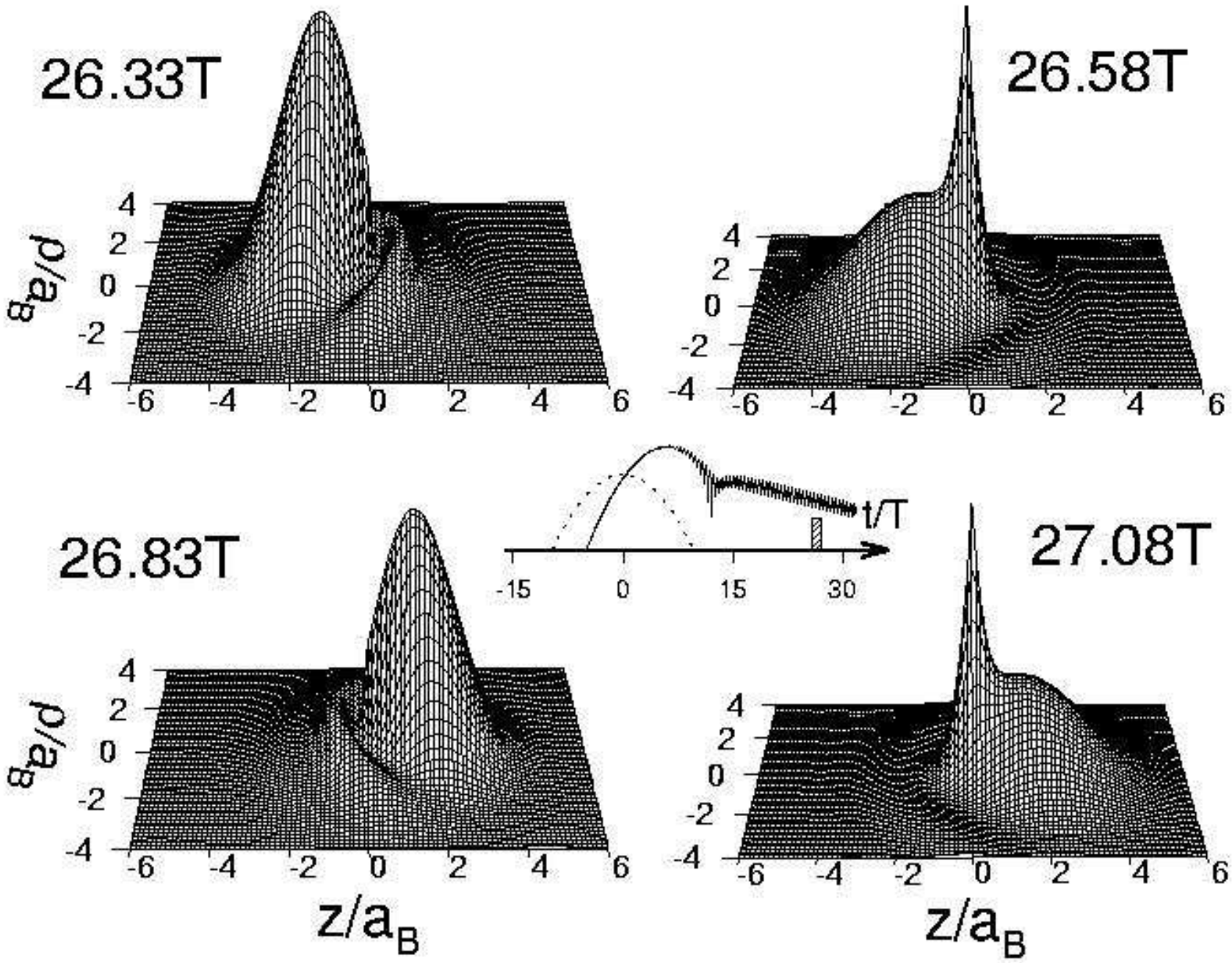
26.33T
26.58T
26.83T
27.08T
ρ/a_B
z/a_B
t/T
4
2
0
-2
-4
-6
-15
15
30